

Intrinsic ^{31}P NMR Chemical Shifts and the Basicities of Phosphate Groups in a Short-Chain Imino Polyphosphate

Hideshi Maki · Masahiko Tsujito · Tetsuji Yamada

Received: 7 June 2012 / Accepted: 27 October 2012 / Published online: 17 May 2013
© The Author(s) 2013. This article is published with open access at Springerlink.com

Abstract The stepwise protonation constants of two linear triphosphate ligand anions, triphosphate, $\text{P}_3\text{O}_{10}^{5-}$ and di-imidotriphosphate, $\text{P}_3\text{O}_8(\text{NH})_2^{5-}$, were investigated by potentiometric titration, and the intrinsic chemical shifts of the stepwise protonated species of these anions were determined from the pH-dependence of the ^{31}P NMR chemical shifts. All stepwise protonation constants of $\text{P}_3\text{O}_8(\text{NH})_2^{5-}$ were found to be larger than those of $\text{P}_3\text{O}_{10}^{5-}$, and the ^{31}P NMR signals due to $\text{P}_3\text{O}_8(\text{NH})_2$ always appeared at a lower magnetic field compared to the signals due to P_3O_{10} . These results indicate higher basicity of the $\text{P}_3\text{O}_8(\text{NH})_2$ ligand, because it contains two imino groups in the ligand molecule. The ^{31}P NMR signals for the end phosphate groups appear at a lower magnetic field than those for the middle phosphate groups, indicating that the basicity of the end phosphate group is higher than that of the middle phosphate group. It can be expected that the high basicity of the $\text{P}_3\text{O}_8(\text{NH})_2$ ligand brings about the formation of high stability complexes with various metal ions. Furthermore, the only ^{31}P NMR signal due to the middle phosphate group of $\text{P}_3\text{O}_8(\text{NH})_2$ ligand molecule clearly showed a low-field shift in the range of $\text{pH} < 2.5$. The reason for this peculiar low-field shift should be the change of the localization of imino protons around the nitrogen atom in $\text{P}_3\text{O}_8(\text{NH})_2$.

Keywords Imido phosphate · Protonation equilibrium · ^{31}P NMR · Potentiometric titration · Imino group · Gran's plot

1 Introduction

The complexation behavior of linear polyphosphate anions, namely the metal complex species and their distribution, is influenced by the effective charge of the anions, which depends on the number of protons bound to the anions. Therefore, the investigation of

H. Maki (✉) · M. Tsujito · T. Yamada
Department of Chemical Science and Engineering, Graduate School of Engineering, Kobe University,
1-1 Rokkodai-cho, Nada-ku, Kobe, Hyougo 657-8501, Japan
e-mail: maki@kobe-u.ac.jp

ligand basicity is important in the study of the complex formation equilibria between linear polyphosphate anions and various metal ions.

The triphosphate anion, $\text{P}_3\text{O}_{10}^{5-}$, is a short-chain polyphosphate anion which consists of three orthophosphate groups (Fig. 1). At least two inflection points are observed during the acid dissociation of long-chain polyphosphate anions, around $\text{pH} = 4.5$ and $\text{pH} = 10$ [1, 2]. This shows that weakly and strongly acidic phosphate groups coexist in these anions. The weakly acidic group is the phosphate group at the center of the ligand molecule, and the strongly acidic groups are the two phosphate groups at the ends of the ligand molecule.

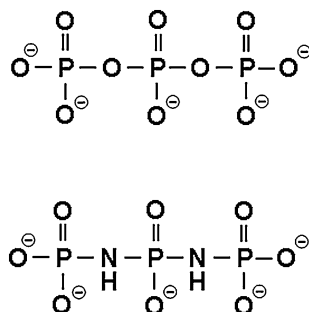
On the other hand, di-imidotriphosphate anion, $\text{P}_3\text{O}_8(\text{NH})_2^{5-}$, is a short-chain imido-polyphosphate anion in which three phosphorus atoms are connected by bridging imino groups (Fig. 1). The main industrial applications of a series of imidophosphates as phosphorus-nitrogen compounds are flame retardants for organic materials [3–9] and solubilizers for medicine [10–14]. The clarification of the protonation equilibria and the estimation of the basicities of the imidophosphates will be useful, since the hydrolysis reactions of the imidophosphates play important parts in these industrial applications. The basicity of P–NH–P binding is higher than that of P–O–P binding [15–18]. Therefore, it can be expected that the stepwise protonation constants of $\text{P}_3\text{O}_8(\text{NH})_2^{5-}$ will be higher than those of $\text{P}_3\text{O}_{10}^{5-}$. In this work, the stepwise protonation constants of $\text{P}_3\text{O}_{10}^{5-}$ and $\text{P}_3\text{O}_8(\text{NH})_2^{5-}$ anions were determined by potentiometric titrations with a Gran's plot [19]. Furthermore, the stepwise protonation constants and the intrinsic chemical shifts of the stepwise protonated species of the anions were determined from the pH-dependence of the ^{31}P NMR chemical shifts. These stepwise protonation constants are applicable to determine the complex formation constants of $\text{P}_3\text{O}_{10}^{5-}$ and $\text{P}_3\text{O}_8(\text{NH})_2^{5-}$ anions. These ligands are monomer analogues of oligophosphate anions, long-chain polyphosphate anions, ultra-phosphate anions, and their imino derivatives. Thus quantitative evaluation of the basicities of the series of these short-chain polyphosphate ligands should provide useful information on the complexation equilibria of these larger anions as well.

2 Experimental

2.1 Chemicals

Pentasodium triphosphate hexahydrate, $\text{Na}_5\text{P}_3\text{O}_{10}\cdot 6\text{H}_2\text{O}$, was synthesized and purified according to the literature [20, 21]. Elemental analysis, calcd: Na, 24.15; P, 19.52; O, 33.62; H_2O , 22.71. Found: Na, 24.52; P, 19.58; O, 33.95; H_2O , 21.95 %. The purity was

Fig. 1 Structures of $\text{P}_3\text{O}_{10-n}(\text{NH})_n^{5-}$ ($n = 0, 2$) anions. Upper $\text{P}_3\text{O}_{10}^{5-}$, lower $\text{P}_3\text{O}_8(\text{NH})_2^{5-}$



obtained by HPLC and ^{31}P NMR measurements, and was found to be over 98 %. As supporting electrolyte, analytical grade of NaNO_3 (Merck Co. Ltd., 99 %) was used without further purification. A standard NaNO_3 stock solution was prepared at about $3.0 \text{ mol}\cdot\text{L}^{-1}$ with distilled water. A portion of the stock solution was dried at $110 \text{ }^\circ\text{C}$ for at least 5 days; the molalities of the stock solution were thus determined gravimetrically. A HNO_3 stock solution was prepared at about $0.25 \text{ mol}\cdot\text{L}^{-1}$ from analytical grade HNO_3 (Wako Pure Chemical Industries, Ltd., 99 %) with distilled water and was standardized by a titration with KHCO_3 [22]. A carbonate-free alkaline stock solution was prepared at about $1.0 \text{ mol}\cdot\text{L}^{-1}$ by dilution of a plastic ampoule of CO_2 -free NaOH aqueous solution (Merck Co. Ltd., No.109959, 99 %) with CO_2 -free water which had been boiled at least 15 min under N_2 atmosphere. The stock solution was checked periodically by Gran's procedure [19], and the carbonate was under 0.5 % of the NaOH present. Other reagents used in this work were analytical grade of ordinary commercial products (over 98 %).

2.2 Preparation of $\text{Na}_5\text{P}_3\text{O}_8(\text{NH})_2\cdot 6\text{H}_2\text{O}$

Pentasodium di-imidotriphosphate hexahydrate, $\text{Na}_5\text{P}_3\text{O}_8(\text{NH})_2\cdot 6\text{H}_2\text{O}$, was synthesized by the improvement of a hydrolysis of trisodium *cyclo*-tri- μ -imidotriphosphate tetrahydrate, $\text{Na}_3\text{P}_3\text{O}_6(\text{NH})_3\cdot 4\text{H}_2\text{O}$, that has been reported [23]. $\text{Na}_3\text{P}_3\text{O}_6(\text{NH})_3\cdot 4\text{H}_2\text{O}$ was synthesized according to the literature [24]. A 10 g sample of $\text{Na}_3\text{P}_3\text{O}_6(\text{NH})_3\cdot 4\text{H}_2\text{O}$ was dissolved in 150 mL of $0.35 \text{ mol}\cdot\text{L}^{-1}$ acetic acid in a three-necked round-bottom flask, and hydrolyzed at $60 \text{ }^\circ\text{C}$ for 16 h with stirring. After cooling to room temperature, the reaction product was precipitated by addition of 150 mL of ethanol. The precipitation was collected by suction filtration, washed with 30 mL of 50 vol% aqueous ethanol, and dissolved in 150 mL of water. A 65 g sample of NaOH pellets was added gradually to the aqueous solution, and the solution was reacted at $70 \text{ }^\circ\text{C}$ for 3 h with stirring. The solution temperature should not be over $75 \text{ }^\circ\text{C}$. After cooling to room temperature, the reaction product was collected by suction filtration, washed with 15 mL of 50 vol% aqueous ethanol and then 30 mL of acetone. This raw $\text{Na}_5\text{P}_3\text{O}_8(\text{NH})_2\cdot 6\text{H}_2\text{O}$ was dissolved in 150 mL of $0.10 \text{ mol}\cdot\text{L}^{-1}$ NaOH aqueous solution, and 12 mL of ethanol was added to the solution. After stirring for several minutes, a white precipitate was collected by suction filtration, washed with 15 mL of ethanol and then 30 mL of acetone. Acetone is more suitable for the final washing than alcohol for the preparation of various inorganic phosphates, since acetone doesn't strongly form hydrogen bonds with the inorganic phosphates. The precipitate was vacuum dried for 1 day, and 1.4 g of pure $\text{Na}_5\text{P}_3\text{O}_8(\text{NH})_2\cdot 6\text{H}_2\text{O}$ was obtained. The total yield was 11 %. Elemental analysis, calcd: Na, 24.25; P, 19.60; O, 27.00; N, 5.91; H_2O , 22.80. Found: Na, 24.84; P, 19.94; O, 27.05; N, 5.79; H_2O , 21.97 %. The purity was obtained by HPLC and ^{31}P NMR measurements, and was found to be over 98 %. The phosphorus concentrations in these ligand stock solutions were determined colorimetrically with a $\text{Mo(V)}\text{--Mo(VI)}$ reagent [25].

2.3 ^{31}P NMR Measurements

All NMR spectra were recorded on a Bruker DPX-250 (5.87T) superconducting Fourier-transform pulse NMR spectrometer with a 10 mm tunable broad-band probe used at 101.258 MHz at $25.0 \pm 1.0 \text{ }^\circ\text{C}$. An acquisition time was 1.0 s, and the FID were collected in 50000 data points, and was used at a sweep width of 25 kHz; that is, the digital resolution in the frequency dimension was 1.0 Hz (0.0099 ppm). In order to avoid saturation of the resonances, the intervals between each FID scan were 5.0 s or more [26]. The NMR chemical

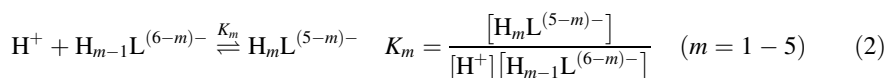
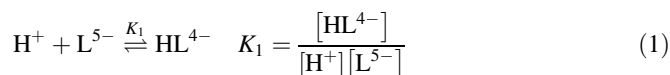
shifts were recorded against an external standard of 85 % H_3PO_4 in 10 % D_2O . Since D_2O was not added to the sample solution, to retain the solvent purity, the spectrometer was not field-frequency locked during the measurement of the sample solutions. All spectra were recorded in the absence of ^1H decoupling. A 3 mL quantity of $0.02 \text{ mol}\cdot\text{L}^{-1} \text{Na}_5\text{P}_3\text{O}_{10}$ or $\text{Na}_5\text{P}_3\text{O}_8(\text{NH})_2 + 1.0 \text{ mol}\cdot\text{L}^{-1} \text{NaNO}_3$ was added to an NMR tube of 10 mm outside diameter, and small aliquots of HNO_3 or NaOH aqueous solution which contained $1.0 \text{ mol}\cdot\text{L}^{-1} \text{NaNO}_3$ was added by a micro syringe in order to control the pH of the solutions. Hence all ^{31}P NMR measurements were performed under constant ionic strength. In this study, all of the sample solutions contain $1.0 \text{ mol}\cdot\text{L}^{-1} \text{NaNO}_3$ as a supporting electrolyte; however, the contribution of the polyphosphate ligands to the total ionic strength is not negligible, hence the ionic strength is not $1.0 \text{ mol}\cdot\text{L}^{-1}$ in the strict sense and contains a slight ambiguity. However, this ambiguity will not negatively impact the results and the findings in this study. The pH meter readings were recorded just before the ^{31}P NMR measurements, and were carried out using an Orion 250A pH meter with a Horiba 6069-10C micro glass electrode. The micro glass electrode was calibrated at pH = (4, 7, and 9) with a phthalate buffer, a phosphate buffer, and a tetraborate buffer, respectively. All ^{31}P NMR measurements were carried out twice, and the measurements showed good agreement with each other.

2.4 Potentiometric Titrations

Stepwise protonation constants of $\text{P}_3\text{O}_{10}^{5-}$ and $\text{P}_3\text{O}_8(\text{NH})_2^{5-}$ anions were determined by potentiometric titrations. All titration procedures were carried out automatically with a personal computer at $25.0 \pm 0.5 \text{ }^\circ\text{C}$ under N_2 atmosphere. A potentiometer (Orion 720A Ionalyzer) equipped with a glass electrode (Orion 91-01) and a single junction reference electrode (Orion 90-02) was used for the potentiometric titrations. 20 cm^3 solutions of $0.02 \text{ mol}\cdot\text{L}^{-1} \text{Na}_5\text{P}_3\text{O}_{10}$ or $\text{Na}_5\text{P}_3\text{O}_8(\text{NH})_2 + 1.0 \text{ mol}\cdot\text{L}^{-1} \text{NaNO}_3$ were titrated stepwise by a solution of $0.01 \text{ mol}\cdot\text{L}^{-1} \text{HNO}_3 + 1.0 \text{ mol}\cdot\text{L}^{-1} \text{NaNO}_3$. Before and after the titrations of the sample solutions, the glass electrode was calibrated as a hydrogen concentration probe by titrating known amounts of HNO_3 with CO_2 -free NaOH solutions, and determining the equivalence point by Gran's method [19] that determines the standard potential, E_0 , and the liquid junction potential, j . These calibrations of the glass electrode were performed under almost the same condition of ionic strength as the titrations for the protonation constants. All titrations were carried out at least 3 times, and all titrations showed good agreement with each other.

2.5 Determination of the Stepwise Protonation Constants

The protonation equilibria for $\text{H}_m\text{P}_3\text{O}_{(10-n)}(\text{NH})_n^{(5-m)-}$ ($m = 0-5$, $n = 0, 2$) that may occur in $\text{Na}_5\text{P}_3\text{O}_{(10-n)}(\text{NH})_n$ ($n = 0, 2$) aqueous solutions and the equations of the mass action law for the equilibria are as follows:



The average number of bound H^+ ions per $\text{H}_m\text{P}_3\text{O}_{(10-n)}(\text{NH})_n^{(5-m)-}$ ($m = 0-5$, $n = 0, 2$), \bar{n} , can be calculated by dividing the concentrations of bound H^+ ions, $[\text{H}^+]_b$, by the total

concentration of ligand ions, C_L . Since $[H^+]_b$ is given as the difference of the total concentration of H^+ ions, C_H , and the free H^+ ion concentration of the equilibrium solution, $[H^+]$, \bar{n} can be determined as:

$$\bar{n} = \frac{[H^+]_b}{C_L} = \frac{(C_H - [H^+])}{C_L} \quad (3)$$

From Eqs. 1–3, \bar{n} can also be expressed as:

$$\bar{n} = \frac{\sum i[H_iL^{(5-i)-}]}{[L^{5-}] + \sum [H_iL^{(5-i)-}]} = \frac{\sum iK_1K_2 \cdots K_i[H^+]^i}{1 + \sum K_1K_2 \cdots K_i[H^+]^i} \quad (i = 5) \quad (4)$$

The stepwise protonation constants of the anions, $\log_{10}K_m$, can be determined from the \bar{n} versus $\log_{10} [H^+]$ plot by a nonlinear least-squares curve-fitting method.

3 Results and Discussion

3.1 Stepwise Protonation Constants of $P_3O_{10-n}(NH)_n^{5-}$ ($n = 0, 2$) by Potentiometric Titration

Figure 2 shows the acid dissociation curves, i.e., the \bar{n} versus $\log_{10} [H^+]$ plots, for $P_3O_{10}^{5-}$ and $P_3O_8(NH)_2^{5-}$ anions. The dissociation curve for $P_3O_8(NH)_2^{5-}$ appears as if the titration curve for $P_3O_{10}^{5-}$ is shifted to the higher pH range. This shows that the proton affinity of the $P_3O_8(NH)_2$ ligand is higher than that of P_3O_{10} ligand [16, 18, 27], because $P_3O_8(NH)_2$ contains imino groups in the molecule [16]. The stepwise protonation constants of the anions, $\log_{10}K_m$, determined by the nonlinear least-squares curve-fitting method are listed in Table 1. The first to third constants can be determined for $P_3O_{10}^{5-}$ and $P_3O_8(NH)_2^{5-}$ and the fourth constant can be determined for $P_3O_8(NH)_2^{5-}$ only. All $\log_{10}K_m$ values of $P_3O_8(NH)_2^{5-}$ were found to be larger than those of $P_3O_{10}^{5-}$, indicating the higher basicity of the $P_3O_8(NH)_2$ ligand. It can thus be expected that $P_3O_8(NH)_2$ forms more stable complexes with various metal ions than P_3O_{10} , because metal cations can be considered as Lewis acids similar to protons.

3.2 ^{31}P NMR Analyses for the Basicities of $P_3O_{10-n}(NH)_n^{5-}$ ($n = 0, 2$) Ligands

The outstanding informative capacity of NMR reveals itself in providing information on an equilibrium system, i.e., determination of a thermodynamic parameter and time-dependent nature of an equilibrium system, as well as providing microscopic information on a molecular structure. In this work, the stepwise protonation constants and the intrinsic chemical shifts of the stepwise protonated species of $P_3O_{10}^{5-}$ and $P_3O_8(NH)_2^{5-}$ anions were determined from the pH profiles of the ^{31}P NMR chemical shifts.

Theoretical considerations of NMR resonances indicate that a qualitative relationship is observed between the NMR chemical shift due to a nucleus and the electronegativity of its neighboring atoms or substituents. Atoms or atomic groups with high electronegativity attract the electronic cloud around a nuclei, so that the magnetic screening for the nuclei is reduced, and the NMR signals due to the nuclei are shifted to lower magnetic field [28–30]. On the other hand, the protonation of the non-bridging oxygen atoms in a ligand causes a

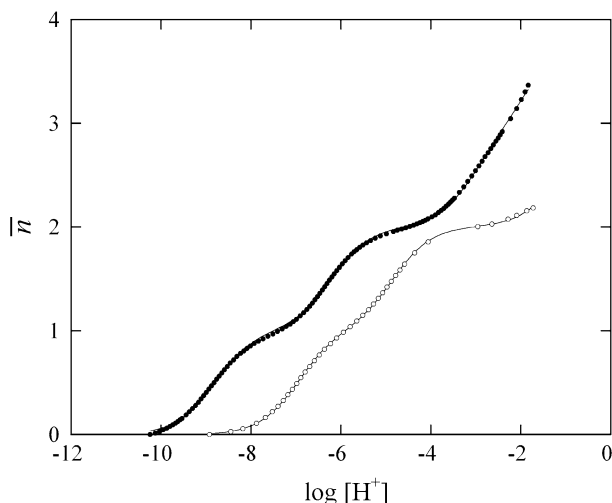


Fig. 2 Potentiometric titration curves of the protonation for $\text{P}_3\text{O}_{10-n}(\text{NH})_n^{5-n-}$ ($n = 0, 2$) anions at 25.0 ± 0.5 °C and $I = 1.0$ mol·L $^{-1}$ (NaNO_3). *Solid lines* refer to the calculated curves by the use of the pertinent parameters of Table 1. *Open circle* $\text{H}_n\text{P}_3\text{O}_{10}^{(5-n)-}$ ($n = 0-3$); *filled circle* $\text{H}_n\text{P}_3\text{O}_8(\text{NH})_2^{(5-n)-}$ ($n = 0-4$)

Table 1 Logarithmic stepwise protonation constants of $\text{P}_3\text{O}_{10-n}(\text{NH})_n^{5-n-}$ ($n = 0, 2$) anions^a determined by potentiometric titrations, $t = 25.0 \pm 0.5$ °C, $I = 1.0$ mol·L $^{-1}$ (NaNO_3)

	$\text{P}_3\text{O}_{10}^{5-}$	$\text{P}_3\text{O}_8(\text{NH})_2^{5-}$
$\log_{10} K_1$	6.96 (< 0.01)	8.80 (0.01)
$\log_{10} K_2$	4.85 (< 0.01)	6.21 (0.01)
$\log_{10} K_3$	1.12 (0.01)	3.02 (0.01)
$\log_{10} K_4$	^{-b}	1.62 (0.01)

^a Values in parentheses indicate standard deviations derived from the nonlinear least-squares approximation

^b Corresponding species were scarcely formed

decrease in the negative charge density of the non-bridging oxygen atom because of the neutralization of negative charge. As a result, the basicity of the phosphate group in a ligand decreases, so that it can be expected that the ^{31}P NMR signal due to the phosphorus nuclei of the phosphate group shifts to higher magnetic field.

The additivity of the chemical shifts of the NMR resonances due to nuclei belonging to the stepwise protonated species, $\text{H}_m\text{L}^{(5-m)-}$ ($m = 0-5$), averaged by fast chemical exchange over all protonated species that are present in the Eqs. 1 and 2 can be expressed in the following form [31]:

$$\delta_{\text{P}} = f_{\text{L}}\delta_{\text{L}} + \sum f_{\text{H}_i\text{L}}\delta_{\text{H}_i\text{L}} \quad (i = 5) \quad (5)$$

where δ_{P} is the observed ^{31}P NMR chemical shift, f_{L} and $f_{\text{H}_i\text{L}}$ are the fraction of each species, and δ_{L} and $\delta_{\text{H}_i\text{L}}$ refer to the intrinsic chemical shifts of the phosphorus nuclei belonging to each species, respectively. Using the mass action law for the stepwise

protonation equilibria, a suitable equation for the observed chemical shift can be expressed as follows:

$$\delta_{\text{P}} = \frac{\delta_{\text{L}} + \sum \left(K_1 K_2 \cdots K_i [\text{H}^+]^i \delta_{\text{H}_i\text{L}} \right)}{1 + \sum \left(K_1 K_2 \cdots K_i [\text{H}^+]^i \right)} \quad (i = 5) \quad (6)$$

The values of the stepwise protonation constants and the intrinsic chemical shifts giving a minimum error-square sum of chemical shifts, $\Sigma(\delta_{\text{P,obs}} - \delta_{\text{P,calc}})^2$, can be determined by a nonlinear least-squares curve-fitting method.

Representative ^{31}P NMR spectra of $\text{Na}_3\text{P}_3\text{O}_{(10-n)}(\text{NH})_n$ ($n = 0, 2$) aqueous solutions are shown in Fig. 3. The $\text{P}_3\text{O}_{(10-n)}(\text{NH})_n$ ($n = 0, 2$) ligands contain two kinds of magnetically non-equivalent phosphorus nuclei, i.e., one nucleus in the phosphate group at the center of a ligand molecule (Mid) and two nuclei in the phosphate groups at the ends of a ligand molecule (End). Therefore, these ligands give a triplet resonance of intensity 1(Mid) and a doublet resonance of intensity 2(End). The pH profiles of the ^{31}P NMR chemical shifts, δ_{P} , of $\text{P}_3\text{O}_{10}^{5-}$ and $\text{P}_3\text{O}_8(\text{NH})_2^{5-}$ anions are shown in Fig. 4, and the stepwise protonation constants and the intrinsic chemical shifts of the stepwise protonated species, determined by the nonlinear least-squares method, are given in Tables 2 and 3, respectively. Table 2 shows that all stepwise protonation constants increased with the increase in the number of imino groups in the ligand, as were the results obtained by potentiometric titration. All stepwise protonation constants obtained from the pH profiles of δ_{P} are similar to those from the potentiometric titrations. However, in a strict comparison, slight differences are found between the protonation constants which were determined by the two techniques. The cause of the slight difference is the calibration condition of the glass electrodes. In the potentiometric titrations, the ionic strength between the calibration solutions and the sample solutions is almost constant; on the other hand, in the ^{31}P NMR measurements, the sample solutions contain $1.0 \text{ mol}\cdot\text{L}^{-1}$ NaNO_3 as supporting electrolyte, but the calibration buffer solutions do not contain a supporting electrolyte at all. Hence the determined protonation constants by ^{31}P NMR include the difference in the activity coefficients of protons. Thus the protonation constants obtained by the potentiometric titrations are preferred.

The ^{31}P NMR signals due to $\text{P}_3\text{O}_8(\text{NH})_2^{5-}$ End and $\text{P}_3\text{O}_8(\text{NH})_2^{5-}$ Mid appeared at lower magnetic field than the signals due to $\text{P}_3\text{O}_{10}^{5-}$ End and $\text{P}_3\text{O}_{10}^{5-}$ Mid, respectively. When the bridging atom in a ligand molecule is changed from oxygen to an imino nitrogen, the following two factors compete in the magnetic shielding for the ^{31}P nucleus:

- (1) an increase of the magnetic shielding for the nucleus based on the decrease of the electronegativity of the bridging atom;
- (2) a decrease of the magnetic shielding for the nucleus based on the decrease of the negative charge density around the phosphorus nuclei, because of the decrease in the number of electrons in the bridging atom.

Although these two factors have opposite effects, the latter effect was found in this work to be stronger than the former, resulting in low-field shift of the ^{31}P NMR signals of $\text{P}_3\text{O}_8(\text{NH})_2$.

On the other hand, as for the comparison of the end and the middle phosphate groups that exist in the same ligand molecule, the ^{31}P NMR signals for the end phosphate groups appear at a lower magnetic field compared to those for the middle phosphate groups, indicating that the basicity of the end phosphate group is higher than that of the middle

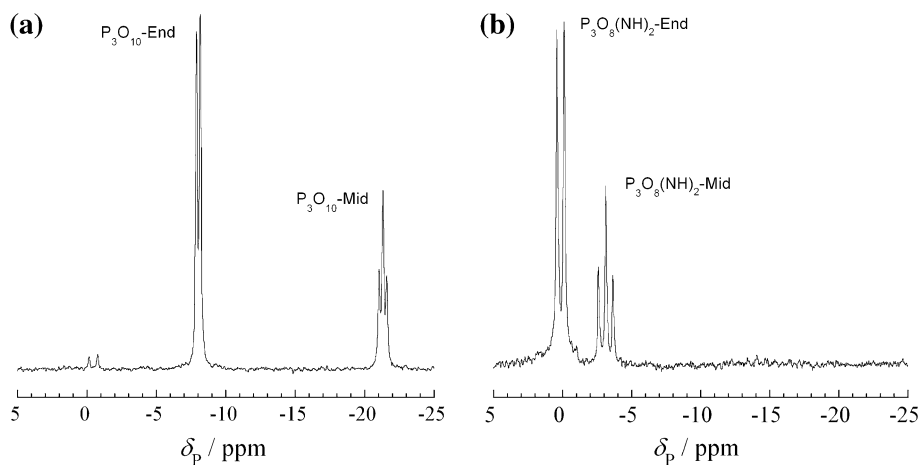
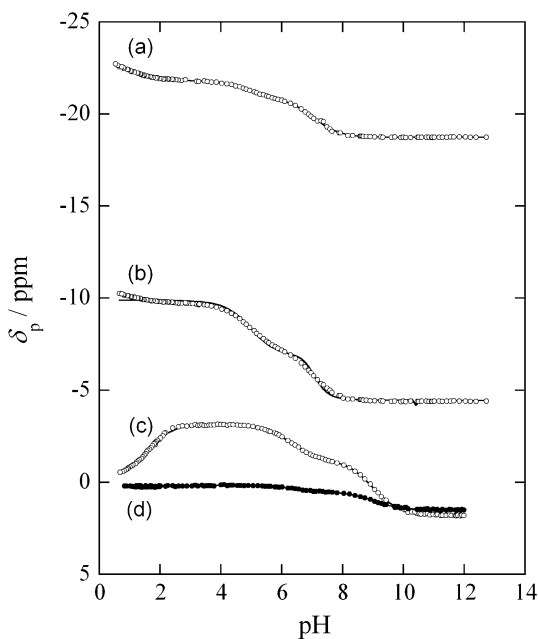


Fig. 3 Representative ^{31}P NMR spectra of $0.02 \text{ mol}\cdot\text{L}^{-1}$ $\text{Na}_5\text{P}_3\text{O}_{10}$ or $\text{Na}_5\text{P}_3\text{O}_8(\text{NH})_2$ aqueous solutions at 101.258 MHz in the absence of ^1H decoupling. **a** $\text{P}_3\text{O}_{10}^{5-}$ anion at $\text{pH} = 5.02$; **b** $\text{P}_3\text{O}_8(\text{NH})_2^{5-}$ anion at $\text{pH} = 4.96$. The details for experimental conditions and each resonance assignment are given in the text

Fig. 4 ^{31}P NMR chemical shifts of $\text{P}_3\text{O}_{10-n}(\text{NH})_n^{5-n-}$ ($n = 0, 2$) anions as a function of pH at $25.0 \pm 1.0 \text{ }^\circ\text{C}$ and $I = 1.0 \text{ mol}\cdot\text{L}^{-1}$ (NaNO_3). Solid lines refer to the calculated curves by the use of the pertinent parameters of Table 2. (a) Middle phosphate groups of $\text{H}_n\text{P}_3\text{O}_{10}^{(5-n)-}$ ($n = 0 - 3$); (b) end phosphate groups of $\text{H}_n\text{P}_3\text{O}_{10}^{(5-n)-}$ ($n = 0 - 3$); (c) middle phosphate groups of $\text{H}_n\text{P}_3\text{O}_8(\text{NH})_2^{(5-n)-}$ ($n = 0 - 4$); (d) end phosphate groups of $\text{H}_n\text{P}_3\text{O}_8(\text{NH})_2^{(5-n)-}$ ($n = 0 - 4$)



phosphate group. The difference in the ^{31}P NMR chemical shifts between the middle and the end phosphorus nuclei is more than 10 ppm over the entire pH range for P_3O_{10} ; however, it is less than 4 ppm for $\text{P}_3\text{O}_8(\text{NH})_2$. This is because of the remarkable low-field shift of the ^{31}P NMR signal of $\text{P}_3\text{O}_8(\text{NH})_2^{5-}$ Mid. This remarkable low-field shift is considered to be caused by the basicity of two neighboring imino nitrogen atoms for $\text{P}_3\text{O}_8(\text{NH})_2^{5-}$ Mid compared to only one neighboring imino nitrogen atom for $\text{P}_3\text{O}_8(\text{NH})_2^{5-}$

Table 2 Logarithmic stepwise protonation constants of $P_3O_{10-n}(NH)_n^{5-}$ ($n = 0, 2$) anions^a determined by the pH profiles of ^{31}P NMR chemical shifts of the anions in aqueous solutions^b, $t = 25.0 \pm 1.0$ °C, $I = 1.0$ mol·L⁻¹ (NaNO₃)

	$P_3O_{10}^{5-}$ End	$P_3O_{10}^{5-}$ Mid	$P_3O_8(NH)_2^{5-}$ End	$P_3O_8(NH)_2^{5-}$ Mid
$\log_{10} K_1$	7.01 (0.01)	7.02 (0.01)	9.05 (0.02)	8.97 (0.01)
$\log_{10} K_2$	4.90 (0.01)	4.82 (0.01)	6.34 (0.04)	6.29 (0.02)
$\log_{10} K_3$	1.09 (0.04)	0.98 (0.04)	3.15 (0.21)	2.96 (0.09)
$\log_{10} K_4$	– ^c	– ^c	– ^d	1.69 (0.02)

^a Values in parentheses indicate standard deviations derived from the nonlinear least-squares approximation

^b In the absence of D₂O for field-frequency locking

^c Corresponding species were scarcely formed

^d This value could not be determined because of the slight change of the ^{31}P NMR chemical shift due to the protonation of the anion

Table 3 Intrinsic ^{31}P NMR chemical shifts of $P_3O_{10-n}(NH)_n^{5-}$ ($n = 0, 2$) anions^a determined by the pH profiles of ^{31}P NMR chemical shifts^b of the anions in aqueous solutions^c, $t = 25.0 \pm 1.0$ °C, $I = 1.0$ mol·L⁻¹ (NaNO₃)

	$P_3O_{10}^{5-}$ End	$P_3O_{10}^{5-}$ Mid	$P_3O_8(NH)_2^{5-}$ End	$P_3O_8(NH)_2^{5-}$ Mid
δ_L^{5-}/ppm	-4.39 (<0.01)	-18.71 (<0.01)	1.53 (0.01)	1.69 (0.02)
δ_{HL}^4/ppm	-7.25 (<0.01)	-20.94 (<0.01)	0.53 (0.01)	-1.19 (0.02)
δ_{H2L}^3/ppm	-9.72 (<0.01)	-21.88 (<0.01)	0.17 (0.01)	-3.16 (0.01)
δ_{H3L}^2/ppm	-10.43 (<0.01)	-23.05 (<0.01)	0.22 (0.01)	-3.01 (0.05)
δ_{H4L}/ppm	– ^d	– ^d	– ^e	-0.30 (0.03)

^a Values in parentheses indicate standard deviations derived from the nonlinear least-squares approximation

^b Referred to external 85 % H₃PO₄

^c In the absence of D₂O for field-frequency locking

^d Corresponding species were scarcely formed

^e This value could not be determined because of the slight change of the ^{31}P NMR chemical shift due to the protonation of the anion

End. In other words, the low-field shift of the ^{31}P NMR signal becomes more significant when more imino nitrogen atoms are adjacent to the phosphorus nuclei.

Approximate quantum chemical calculations [32, 33] have shown that the change in the chemical shift, $\Delta\delta$, for the anions may be treated by the relationship [34–36]:

$$\Delta\delta = 180\Delta\chi_0 - 147\Delta n_\pi - A\Delta\theta \quad (7)$$

where $\Delta\chi_0$ is the change in the effective electronegativity of the phosphorus atom, Δn_π is the concomitant change in the phosphorus d_π -orbital occupation due to variation in the π character of the P–X bonds thus induced, $\Delta\theta$ is the change in the bond angle, and A is an arbitrary parameter to accommodate variations between oxoacids. Thus the change in electronegativity, $\Delta\chi_0$, which originates from the decrease in negative charge with protonation, certainly predominates for the upfield shifts observed for the phosphorus nuclei in $H_mP_3O_{(10-n)}(NH)_n^{(5-m)-}$ ($m = 0-3$, $n = 0, 2$) anions. However, the only ^{31}P NMR signal due to $P_3O_8(NH)_2^{5-}$ Mid clearly showed a low-field shift in the range of pH < 2.5. This peculiar low-field shift leads us to consider an important aspect in the change of the

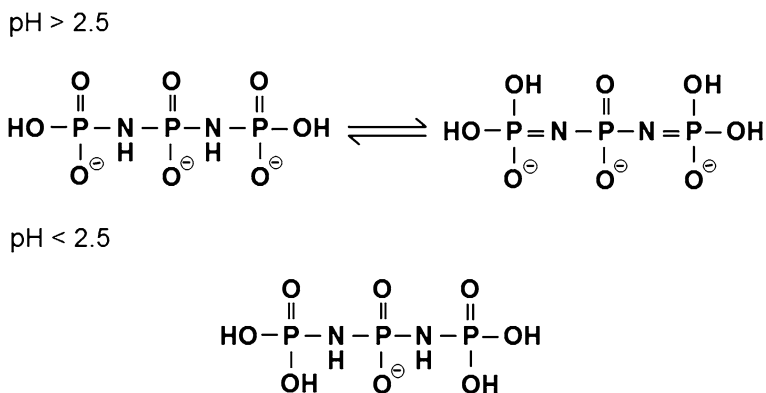


Fig. 5 Tautomerism of a di-imidotriphosphate molecule in the range of pH > 2.5

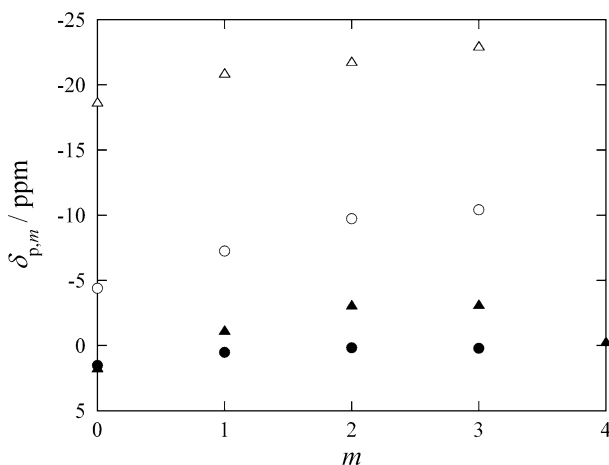


Fig. 6 Correlation of the intrinsic ^{31}P NMR chemical shifts of $\text{P}_3\text{O}_{10-n}(\text{NH})_n^{5-}$ ($n = 0, 2$) anions and the number of binding protons to the anions. *Open triangle* middle phosphate groups of $\text{H}_n\text{P}_3\text{O}_{10}^{(5-n)-}$ ($n = 0-3$); *open circle* end phosphate groups of $\text{H}_n\text{P}_3\text{O}_{10}^{(5-n)-}$ ($n = 0-3$); *filled triangle* middle phosphate groups of $\text{H}_n\text{P}_3\text{O}_8(\text{NH})_2^{(5-n)-}$ ($n = 0-4$); *filled circle* end phosphate groups of $\text{H}_n\text{P}_3\text{O}_8(\text{NH})_2^{(5-n)-}$ ($n = 0-4$)

localization of imino protons in $\text{P}_3\text{O}_8(\text{NH})_2$ anions, i.e., tautomerism of the molecules as shown in Fig. 5. Imino protons in the ligand will not be localized around the imino nitrogen atom owing to the tautomerism in the range of pH > 2.5. The tautomerism is observed as if the intermolecular hydrogen bonding between the bridging nitrogen atoms and the nonbridging oxygen atoms occurs in the NMR time scale. On the other hand, in the range of pH < 2.5, the localization of imino protons around the nitrogen atom owing to the deceleration of the tautomerism will be greatly accelerated by the progress of successive protonations of the non-bridging oxygen atoms. Thus the change of the localization of imino protons in $\text{P}_3\text{O}_8(\text{NH})_2$ ligand causes a change in the N–P–N bond angle. Therefore, the ^{31}P NMR signal due to $\text{P}_3\text{O}_{10-n}(\text{NH})_n^{5-}$ Mid shows a drastic downfield shift with successive protonations because of the change in the N–P–N bond angle, i.e., the contribution of the $\Delta\theta$ term in Eq. 7. The intrinsic ^{31}P NMR chemical shift values due to the

stepwise protonated species, δ_P , m , are plotted against the number of binding protons to the ligands, m , as shown in Fig. 6. Low-field shifts in the ^{31}P NMR signals were observed as the number of imino nitrogen adjacent to the phosphorous atom increased. The high basicity of the $\text{P}_3\text{O}_8(\text{NH})_2$ ligand will bring about the formation of high stability complexes with various metal ions.

4 Conclusions

All stepwise protonation constants of $\text{P}_3\text{O}_8(\text{NH})_2^{5-}$ anions were found to be larger than those of $\text{P}_3\text{O}_{10}^{5-}$ anions, because $\text{P}_3\text{O}_8(\text{NH})_2$ contains two imino groups. The ^{31}P NMR signals due to phosphorus nuclei in the end phosphate groups appear at a lower magnetic field than those in the middle phosphate groups, showing that the basicity of the end phosphate groups is higher than that of the middle phosphate groups. The ^{31}P NMR signals of $\text{P}_3\text{O}_8(\text{NH})_2$ appear at a lower magnetic field compared to those of P_3O_{10} due to both the middle and the end phosphate groups, indicating that the basicity of $\text{P}_3\text{O}_8(\text{NH})_2$ ligand is higher than that of P_3O_{10} ligand. The high basicity of the imino group was confirmed by potentiometric titrations with an electrochemical method and by ^{31}P NMR spectra as a spectroscopic method. As a consequence, the $\text{P}_3\text{O}_8(\text{NH})_2$ ligand is expected to exhibit higher H^+ ion binding ability compared with the P_3O_{10} ligand, and also to form stable complexes with various metal ions. The complexation equilibria between various metal ions and these ligands are expected to be influenced by the decrease of the negative charge of these ligands due to protonation of the ligands in the low pH range. The protonation constants of $\text{P}_3\text{O}_{10}^{5-}$ and $\text{P}_3\text{O}_8(\text{NH})_2^{5-}$ anions determined in this work can be applied to the accurate estimation of the complex formation constants of these ligands.

Acknowledgments The authors express grateful acknowledgement to Prof. Makoto Watanabe (Department of Industrial Chemistry, Chubu University, Japan) and Ph.D. Makoto Sakurai for preparation of pentasodium di-imidotriphosphate hexahydrate, $\text{Na}_5\text{P}_3\text{O}_8(\text{NH})_2 \cdot 6\text{H}_2\text{O}$.

Open Access This article is distributed under the terms of the Creative Commons Attribution License which permits any use, distribution, and reproduction in any medium, provided the original author(s) and the source are credited.

References

1. Van Wazer, J.R., Griffith, E.J., McCullough, J.F.: Analysis of phosphorus compounds; Automatic pH titration of soluble phosphates and their mixtures. *Anal. Chem.* **26**, 1755–1759 (1954)
2. Miyajima, T., Yamauchi, K., Ohashi, S.: Characterization of inorganic long-chain polyphosphate by a sephadex G-100 column combined with an autoanalyzer detector. *J. Liq. Chromatogr.* **4**, 1891–1901 (1981)
3. Fei, S., Allcock, H.R.: Methoxyethoxyethoxyphosphazenes as ionic conductive fire retardant additives for lithium battery systems. *J. Power Sources* **195**, 2082–2088 (2010)
4. Lu, S., Hamerton, I.: Recent developments in the chemistry of halogen-free flame retardant polymers. *Prog. Polym. Sci.* **27**, 1661–1712 (2002)
5. Liu, R., Wang, X.: Synthesis, characterization, thermal properties and flame retardancy of a novel nonflammable phosphazene-based epoxy resin. *Polym. Degrad. Stab.* **94**, 617–624 (2009)
6. Gouri, M.E., Bachiri, A.E., Hegazi, S.E., Rafik, M., Harfi, A.E.: Thermal degradation of a reactive flame retardant based on cyclotriphosphazene and its blend with DGEBA epoxy resin. *Polym. Degrad. Stab.* **94**, 2101–2106 (2009)

7. Gleria, M., Bertani, R., Jaeger, R.D., Lora, S.: Fluorine containing phosphazene polymers. *J. Fluorine Chem.* **125**, 329–337 (2009)
8. Shin, Y.J., Ham, Y.R., Kim, S.H., Lee, D.H., Kim, S.B., Park, C.S., Yoo, Y.M., Kim, J.G., Kwon, S.H., Shin, J.S.: Application of cyclophosphazene derivatives as flame retardants for ABS. *J. Ind. Eng. Chem.* **16**, 364–367 (2010)
9. Çoşut, B., Hacivelioglu, F., Durmuş, M., Kılıç, A., Yeşilot, S.: The synthesis, thermal and photo-physical properties of phenoxycyclotriphosphazeny-substituted cyclic and polymeric phosphazenes. *Polyhedron* **28**, 2510–2516 (2009)
10. Inoue, H., Nakayama, H., Tshako, M., Maki, H., Nariai, H., Eguchi, T.: Phosphorylation of methylamine with inorganic monoimido-*cyclo*-triphosphate. *Phosphorus Res. Bull.* **17**, 170–173 (2004)
11. Inoue, H., Kawashita, T., Nakayama, H., Tshako, M.: Regioselective phosphorylation of branched cyclodextrins with *cyclo*-mono- μ -imidotriphosphate. *Carbohydr. Res.* **340**, 1766–1772 (2005)
12. Inoue, H., Nakayama, H., Nariai, H., Tshako, M.: Syntheses of organic phosphorus compounds with –NH–P–NH– and –NH–P–O– bonds by inorganic monoimido-*cyclo*-triphosphate. *Phosphorus Res. Bull.* **19**, 319–324 (2005)
13. Inoue, H., Yamada, T., Nakayama, H., Tshako, M.: Phosphorylation of D-glucose derivatives with inorganic monoimido-*cyclo*-triphosphate. *Chem. Pharm. Bull.* **54**, 1397–1402 (2006)
14. Maeda, H., Chiba, T., Tshako, M., Nakayama, H.: Phosphorylation of nucleosides and nucleotides with inorganic monoimido-*cyclo*-triphosphate. *Chem. Pharm. Bull.* **56**, 1698–1703 (2008)
15. Smith, R.M., Martell, A.E.: *Critical Stability Constants, Inorganic Complexes*. Plenum Press, New York (1976)
16. Miyajima, T., Maki, H., Sakurai, M., Watanabe, M.: On the protonation equilibria of *cyclo*- μ -imidopoliphosphate anions(I). *Phosphorus Res. Bull.* **5**, 149–154 (1995)
17. Miyajima, T., Maki, H., Sakurai, M., Watanabe, M.: On the protonation equilibria of *cyclo*- μ -imidopoliphosphate anions(II). *Phosphorus Res. Bull.* **5**, 155–160 (1995)
18. Maki, H., Nariai, H., Miyajima, T.: ^9Be and ^{31}P NMR analyses on Be^{2+} complexation with *cyclo*-tri- μ -imido triphosphate anions in aqueous solution. *Polyhedron* **30**, 903–912 (2011)
19. Gran, G.: Determination of the equivalence point in potentiometric titrations. Part II. *Analyst* **77**, 661–671 (1952)
20. Watanabe, M., Matsuura, M., Yamada, T.: The mechanism of the hydrolysis of polyphosphates. V. The effect of cations on the hydrolysis of pyro- and triphosphates. *Bull. Chem. Soc. Jpn.* **54**, 738–741 (1981)
21. Audrieth, L.F.: *Inorganic Syntheses*. McGraw-Hill, New York (1950)
22. Ootaki, H.: The practical guide for potentiometry. *Denki Kagaku* **44**, 151–156 (1976)
23. Watanabe, M., Hinatase, M., Sakurai, M., Sato, S.: The synthesis and thermal property of sodium diimidotriphosphate. *Gypsum Lime* **232**, 146–150 (1991)
24. Watanabe, M., Sakurai, M., Hinatase, M., Sato, S.: Synthesis and thermal property of sodium triimidocyclotriphosphate. *J. Mater. Sci.* **27**, 743–746 (1992)
25. Conde, F.L., Prat, L.: A new reagent for the colorimetric and spectrophotometric determination of phosphorus, arsenic and germanium. *Anal. Chim. Acta* **16**, 473–479 (1957)
26. Braun, S., Kalinowski, H.O., Berger, S.: *150 and More Basic NMR Experiments: A Practical Course*. Wiley-VCH, Weinheim (1998)
27. Maki, H., Ueda, Y., Nariai, H.: Protonation equilibria and stepwise hydrolysis behavior of a series of thiomonophosphate anions. *J. Phys. Chem. B.* **115**, 3571–3577 (2011)
28. Harris, R.K.: *Nuclear Magnetic Resonance Spectroscopy*. Longman, London (1986)
29. Jameson, C.J., Gutowsky, H.S.: Calculation of chemical shifts. I. General formulation and the Z dependence. *J. Chem. Phys.* **40**, 1714–1724 (1964)
30. Akitt, J.W.: *NMR and Chemistry: An Introduction to Modern NMR Spectroscopy*, Chap. 2.1. Chapman & Hall, London (1992)
31. Kudryavtsev, A.B., Linert, W.: *Physico-chemical Applications of NMR: A Practical Guide*. World Scientific Publishing Co. Pte. Ltd., Singapore (1996)
32. Letcher, J.H., Van Wazer, J.R.: Theoretical interpretation of ^{31}P NMR chemical shifts. I. *J. Chem. Phys.* **44**, 815–829 (1966)
33. Letcher, J.H., Van Wazer, J.R.: Theoretical interpretation of ^{31}P NMR chemical shifts. II. Unsymmetrical molecules. *J. Chem. Phys.* **45**, 2916–2925 (1966)
34. Moedritzer, K.: pH dependence of phosphorus-31 chemical shifts and coupling constants of some oxyacids of phosphorus. *Inorg. Chem.* **6**, 936–939 (1967)
35. Haake, P., Prigodich, R.V.: Method for determination of phosphate anion–cation association constants from ^{31}P chemical shifts. *Inorg. Chem.* **23**, 457–462 (1984)
36. Costello, A.J.R., Glonek, T., Van Wazer, J.R.: Phosphorus-31 chemical shift variations with counterion and ionic strength for the various ethyl phosphates. *Inorg. Chem.* **15**, 972–974 (1976)